polymers

MDPI

Article

Study into the Mechanical Properties of a New Aeronautic-Grade Epoxy-Based Carbon-Fiber-Reinforced Vitrimer

Cristian Builes Cárdenas [1,*], Vincent Gayraud [1], Maria Eugenia Rodriguez [1,*], Josep Costa [2], Asier M. Salaberria [3], Alaitz Ruiz de Luzuriaga [3], Nerea Markaide [3], Priya Dasan Keeryadath [4] and Diego Calderón Zapatería [5]

[1] Composites Unit, Eurecat—Technological Center of Catalonia, 08290 Cerdanyola del Valles, Spain; vincent.gayraud@eurecat.org
[2] Analysis and Advanced Materials for Structural Design (AMADE), Polytechnic School, Campus Montilivi, University of Girona, 17071 Girona, Spain; josep.costa@udg.edu
[3] CIDETEC, Basque Research and Technology Alliance (BRTA), Paseo Miramón, 196, 20014 Donostia-San Sebastian, Spain; amartinez@cidetec.es (A.M.S.); aruiz@cidetec.es (A.R.d.L.); nmarkaide@cidetec.es (N.M.)
[4] ÉireComposites Teo, An Choill Rua, H91Y923 Inverin, County Galway, Ireland; info@eirecomposites.com
[5] IDEC, Engineering Composites Advanced Solution. C/Albert Einstein 29, 01510 Minano Menor, Spain; d.calderon@idec.aero
* Correspondence: cristian.builes@eurecat.org (C.B.C.); meugenia.rodriguez@eurecat.org (M.E.R.)

Abstract: The current drive for sustainability demands recyclable matrices for composite materials. Vitrimers combine thermoset properties with reprocessability, but their mechanical performance in highly loaded applications, for instance, composites for aeronautics, is still to be demonstrated. This work presents the complete mechanical characterization of a new vitrimer reinforced with carbon fiber. This vitrimer formulation consists of functional epoxy groups and a new dynamic disulfide crosslinks-based hardener. The testing campaign for the vitrimer composites encompassed tension, compression, interlaminar shear strength (ILSS), in-plane shear (IPS), open-hole tension (OHT) and compression (OHC), filled-hole compression (FHC) and interlaminar fracture toughness tests under mode I and II. Test conditions included room temperature and high temperature of 70 °C and 120 °C, respectively, after moisture saturation. Tension and flexural tests also were applied on the neat vitrimer resin. The results compared well with those obtained for current aeronautic materials manufactured by Resin Transfer Molding (RTM). The lower values observed in compression and ILSS derived from the thermoplastic veils included as a toughening material. This work demonstrates that the vitrimer formulation presented meets the requirements of current matrices for aeronautic-grade carbon-reinforced composites.

Keywords: vitrimers; carbon fiber composites; aeronautical industry; mechanical properties

Citation: Builes Cárdenas, C.; Gayraud, V.; Rodriguez, M.E.; Costa, J.; Salaberria, A.M.; Ruiz de Luzuriaga, A.; Markaide, N.; Dasan Keeryadath, P.; Calderón Zapatería, D. Study Into the Mechanical Properties of a New Aeronautic-Grade Epoxy-Based Carbon-Fiber-Reinforced Vitrimer. *Polymers* **2022**, *14*, 1223. https://doi.org/10.3390/polym14061223

Academic Editors: John Vakros, Evroula Hapeshi, Catia Cannilla and Giuseppe Bonura

Received: 31 January 2022
Accepted: 14 March 2022
Published: 17 March 2022

1. Introduction

Thermoset fiber-reinforced composites have been widely used in numerous structural applications, particularly in the aerospace, automotive and wind power industries. Epoxies have excellent thermal and dimensional stability, good mechanical strength, creep and chemical resistance and good electrical isolation thanks to their permanent covalent cross-linked networks. That said, thermosets have long curing times, thus limiting their production to low-medium volume series, for which there is an increasing demand. In addition, thermosets have poor or complex reparability, are non-recyclable and cannot be reshaped after being cured, therefore generating a great deal of waste when components reach the end of their lifespans. The current and most common disposal solutions are pyrolysis and land filling, both of which imply serious environmental and economic issues [1–7].

Back in 2011, Leibler et al. [8] presented a new kind of polymer with outstanding properties called covalent adaptative networks (CANs), dynamers or vitrimers that combine the performance of traditional thermosets with the versatility of thermoplastics due to characteristics such as processability, weldability, self-healing capacity and recyclability. Vitrimers, having associative dynamic networks, behave like traditional thermoset resins at service temperatures due to their frozen network topology. However, under certain stimuli, such as heat or light, they are able to reorganize their networks while maintaining a constant number of chemical bonds. The dissociative formulations reduce network crosslinking density, thus diminishing polymer dimensional stability and viscosity during reprocessing. Some vitrimer formulations need the addition of external catalysts to create the bond exchange reactions, as the material is heated above the vitrimeric transition temperature, therefore presenting issues with vitrimer stability, manipulation and mechanical response. Some studies present new formulations of catalyst-free vitrimers that can be processed with commercially available precursors, maintaining their properties during reprocessing and are more easily implemented on an industrial scale [2,9–19].]

Vitrimers present new possibilities for fiber-reinforced polymers such as post-curing reprocessing without losing performance, welding composite layers to form new monolithic and multi-layered materials or allowing composites to be welded to generate structural joints between parts. Additionally, the fibers and the matrix can be separated for reuse in other applications. Furthermore, vitrimers allow for the implementation of "enduring" prepregs that could be fully cured and still enable the processing of multi-layered laminates, thus avoiding the need for refrigerated storage and the multiple consumable materials for prepreg protection, in addition to offering a longer shelf life. Vitrimers offer the potential to create reprocessable and reparable thermoset composites, something which currently is a slow and expensive process requiring highly qualified personnel [9,11,20–24].

A pioneering publication on fiber-reinforced vitrimers by A. Ruiz de Luzuriaga et al. [9] presented a glass-fiber-reinforced vitrimer based on diglycidyl ether of bisphenol A (DGEBA) epoxy monomer and a 4-aminophenyl disulfide dynamic hardener. This is a catalyst-free formulation that presents fast stress relaxation at high temperatures. Compared to a traditional DGEBA epoxy with diethyltoluenediamine (DETDA, 2) hardener, the disulfide vitrimer showed comparable values of glass transition temperature (T_g), storage modulus (E') and thermal stability, albeit with a slightly lower degradation temperature (T_d), possibly due to the disulfide species that are less energetically stable than other species in the formulation. Both the vitrimer and the thermoset showed comparable traction strength, suggesting that the use of dynamic formulations on composites will not affect their mechanical performance. The authors demonstrated the possibility of reshaping a cured composite sample manufactured by RTM and thermoforming it in a hot press. The reparability of the vitrimer formulation was illustrated by inducing delamination during an ILSS test and healing it by means of heating and pressure.

Over the past years, several vitrimer composites with diverse synthetic or natural monomers and dynamic formulations have been applied in continuous glass or carbon fiber reinforcements, showing promising mechanical properties compared to their thermoset counterparts [6,10,19,20,23,25–37]. Some vitrimer formulations have attractive properties such as a high tensile strength, interlaminar shear strength or glass transition temperatures [6,23]. However, there is still a gap between their performance and current aerospace-grade structural thermoset composites (as displayed in Table 1), with no reported aerospace-capable vitrimer formulations yet. No detailed mechanical studies on vitrimer-based composites relevant to the aviation industry are available for use in evaluating the possible implementation of high-performance fiber-reinforced vitrimers in real structures.

Table 1. Summary of reported properties for vitrimer composites and some thermoset aeronautic-grade references.

Reference	Fiber/Fabric	Resin/Monomer	Dynamic System/Hardener	Tensile Modulus [GPa]	Tensile Strength [MPa]	Compression Strength [MPa]	Flexural Modulus [GPa]	Flexural Strength [MPa]	ILSS [MPa]	Impact Strength [kJ/m²]	Tg [°C]
A. Ruiz et al. [9]	Glass	Diglycidyl ether of bisphenol A	4-aminophenyl disulfide	-	-	292 ± 16	-	595 ± 39	37 ± 3	194 ± 18	130
W. Denissen et al. [25], [26]	Glass—plain weave (hot-pressed)	Vinylogous urethane	Amine	33.2	336	-	-	-	-	-	-
X. Liu et al. [32]	Glass cloth (180 g/m²)	Phenol formaldehyde	Urethane	-	-	-	-	184.1	12.93	-	157
H. Si et al. [10]	Carbon	Bis(4-glycidyloxyphenyl) disulfide	4-aminophenyl disul-fide	10.5	334.5 ± 87.7	-	-	-	-	-	147
Y. Yuan et al. [6]	Carbon woven T300-1000 (119 g/m²)	Poly(hexahydrotriazine)	2,2-bis[4-(4-aminophenoxy) phenyl]propane	68.3	741.2	351.5	54.8	829.7	75.5	-	198.2
	Carbon UD HS (200 g/m²)			141.7	1806.6	343.3	127.4	1241.2	69.1	-	199.5
P. Taynton et al. [28]	Carbon—twill weave	Diamine	Polyimine	14.2 ± 1.1	399 ± 85	-	32.4 ± 3.7	255 ± 56	-	-	145
S. Wang et al. [31]	Carbon	Phenol formaldehyde	Boronic ester	-	-	-	24.2 ± 0.3	411.6 ± 5.3	48 ± 2.5	-	153
Y. Liu et al. [19]	Carbon	Itaconic acid-based epoxy	Maleic acid + glycerin	31.3	417	-	-	-	45	-	54
S. Wang et al. [23]	Carbon—plain weave	Vanillin epoxy	Diamine 4,4′-methyl-enebiscyclohexanamine	35.3 ± 2.4	763 ± 71	-	-	-	-	-	172
Y. Y. Liu et al. [35]	Carbon	Bio epoxidized soybean oil	Vanillin + 4-aminophenol	1.18 ± 0.14	145.4 ± 17.13	-	-	-	-	-	27.6
Y. Y. Liu et al. [36]	Carbon—plain weave	Glycerol triglycidyl ether	Vanillin + A4-aminophenol	12.9	449	-	-	-	-	-	70

H. Memom et al. [20]	Carbon	Trifunctional epoxy	Vanillin + methylcyclohexanediamine	-	-	-	56	1028	52	-	131
T. Liu et al. [33]	Carbon	Bisphenol A + Ethylenediamine	Glutaric anhydride	17.1 ± 2.5	356 ± 28.7	-	-	-	-	-	95
H. Wang et al. [34]	Carbon (low wt%)	Diglycidyl ether of bisphenol F	4-Aminophenyl disulfide + γ-Aminopropyltriethoxysilane + Poly(propylene glycol) bis(2-aminopropyl ether)	10.18	320	-	-	-	-	-	97.4
Y. Xu et al. [37]	Carbon (braided 60% FVF)	Epoxidized menthane diamine	Adipic acid	-	465	-	-	-	-	-	86.4
Aeronautic standard reference [6]	Carbon–5h satin (prepreg)	Hexply 914	-	70	631	-	61	912	64	-	190
Aeronautic standard reference [38]	Carbon 8H satin 6K (prepreg)	Hexply 8552	-	86	1014	-	-	-	90	-	200
Aeronautic standard reference [39]	Carbon UD (prepreg)	Epikote 475	-	-	-	-	60	1020	65	-	190
Aeronautic standard reference (approximated results) [40]	Carbon–5H satin (370 g/m^2)	RTM6	-	69	1180	950	-	-	67.5	-	-

The EU H2020 project AIRPOXY (thermoformAble, repaIrable and bondable smaRt ePOXY-based composites for aero structures) [41,42] was funded with the aim of introducing vitrimer advantages into the aeronautic industry to reduce production and maintenance costs of aeronautic composite parts. Vitrimer-based composites offer new properties such as reprocessability, reparability and recyclability, while still maintaining high-performance.

This work is developed as part of the AIRPOXY project, and its objective is to present a full mechanical characterization of a new carbon-fiber-reinforced vitrimer based on disulfide exchange bonds, designed to compete in performance with current and widely used aerospace-grade thermoset epoxy resins. In this paper, we focus on composite properties; details of the vitrimer formulation and its properties will be published in separate works under the Airpoxy project. Two reinforcement configurations were selected and evaluated under different mechanical tests at room temperature and in humidity and high-temperature conditions to obtain a full spectrum of this vitrimer formulation's mechanical performance. We present a description of the mechanical tests selected, along with their outcomes, materials and manufacturing processes. Following that, we present a discussion on the results and draw some conclusions.

2. Experimental

2.1. Materials

We used a new formulation of an aeronautical-grade epoxy-based vitrimer (referred to from here on as AIR-3R) that has low viscosity at processing temperatures so that it can be processed by infusion and RTM processes. It consists of a catalyst-free formulation composed of commercially available functional epoxy groups and a new hardener with dynamic crosslinks based on aromatic disulfide species, also commercially available. This is a patented formulation, created, characterized and provided by Cidetec (Donostia—San Sebastián, Spain) [43–45].

Two different carbon fiber reinforcements provided by Chomarat (Le Cheylard, France) were used in this study. One was C-WEAVE™ 280SA5 (Figure 1a), which is 5-harness satin (5HS) woven fabric with T800HB 6K (Chomarat) intermediate modulus fibers and an aerial weight of 280 g/m^2 [46]. The other reinforcement was C-PLY™ SP U268S5 (Chomarat) (Figure 1b), which is a unidirectional (UD) fabric with T800H 24K intermediate modulus fibers and an aerial weight of 284 g/m^2. Both reinforcements were manufactured with a custom-made polyamide (PA) stabilization veil (Chomarat) with an aerial weight of 8 g/m^2, intended to improve the interlaminar toughness of the final vitrimer composites. (Figure 1c). The fiber volume content (FVC) for both vitrimer composites and thermoset baseline reference was set to 58%, considering the fabrics characteristics, samples thickness and number of fabric plies [47,48].

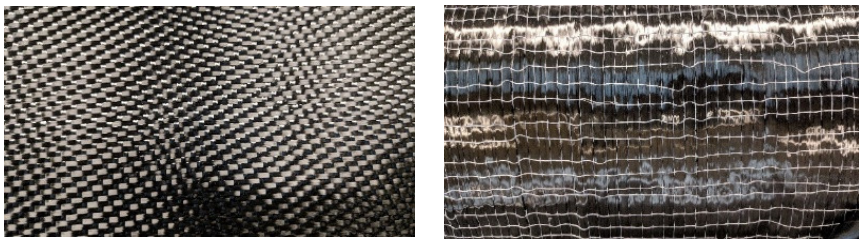

(**a**) (**b**)

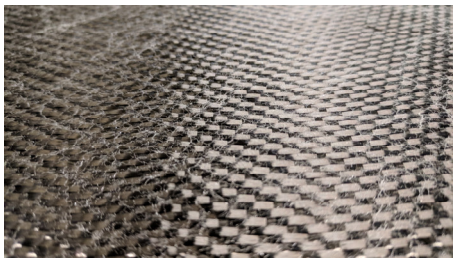

(**c**)

Figure 1. Fabric reinforcement structures used in this study. (**a**) 5-Harness satin weave. (**b**) UD fabric. (**c**) Detail of PA binder veil.

To characterize the 5HS fabric, we tested cross-ply configurations (CP), while for the UD reinforcement, 0° and 90° configurations were used. Laminate tests were performed over a quasi-isotropic configuration (Table 2).

Table 2. Baseline specifications for the AIR-3R resin based on conventional STD-AR. Adapted from [47].

Material	**Specification**	**Unit**	**Value**					
Neat resin	Glass transition temperature	°C	>170					
	Tensile modulus	GPa	3					
	Tensile strength	MPa	75					
	Flexural modulus	GPa	3.3					
	Flexural strength	MPa	132					
Material	**Specification**	**Unit**	**Fabric configuration and test conditioning**					
			CP			**UD**		
			RT	**HW70**	**HW120**	**RT**	**HW70**	**HW120**
Ply properties	Tensile modulus—warp direction	GPa		>70			>155	
	Tensile modulus—weft direction	GPa		>70			>8.5	
	Tensile strength—warp direction	MPa		>980			>2325	
	Tensile strength—weft direction	MPa		>980			>47.6	
	Compression modulus—warp direction	GPa		>68			>140	
	Compression modulus—weft direction	GPa		>68			>8.5	
	Compression strength—warp direction	MPa		>646			>1386	
	Compression strength—weft direction	MPa		>646			>255	
	Interlaminar shear strength	MPa	>60	>42	>30	>70	>42	>30
	In-plane shear modulus	GPa	>4.5	>3.6	>2.3	>4.4	>3.5	>2.2
	In-plane shear strength	MPa	>86	>73	>49	>82	>65	>41
Material	**Specification**	**Unit**	**Quasi-isotropic laminate**					

			RT	HW70	HW120
Laminate properties	Fracture toughness G_{IC} *	J/m²		>700	
	OHT strength	MPa	>490	>380	>360
	OHC strength	MPa	>340	>250	>180
	FCH strength	MPa	>430	>300	>275

* Fracture toughness mode II (G_{IIC}) is not available on the baseline data.

Materials were tested as received at room temperature (RT) or preconditioned until equilibrium at 70 °C and 85% relative humidity (RH) and then tested at two different temperatures, 70 °C (HW70) and 120 °C (HW120).

Open-hole tension and compression and filled-hole Compression tests were carried out at RT and HW70 conditions. Interlaminar fracture toughness tests were conducted at RT.

2.2. Manufacturing Procedure

Panels were prepared by RTM using three-part metallic molds: upper and lower mold parts with an intermediate spacer, which gives the samples their final thickness required for the mechanical tests. Cavity dimensions were 505 mm × 605 mm for a steel mold and 380 mm × 220 mm for an aluminum mold. One of the two molds was selected depending on the test preparation, specimen dimensions or availability. Both were heated with an oil-based electric heater Tool Temp TT-380 (Tool Temp. Rubí, Spain) of 32 kW capacity. Injection was carried out on a Coexpair Injector 5000cc RTM machine (Coexpair. Namur, Belgium).

Dry fabrics were cut and manually placed inside the mold cavity with the specific reinforcement type and stacking sequence for each test. No pressure or temperature change was applied to the laminate during the preforming process, as displayed in Figure 2a. Injection was carried out at a constant rate of 50 g/min, maintaining a maximum pressure of 1 bar. When the mold cavity was full, a post-filling step was applied, thus increasing the cavity pressure up to 4 bars to ensure full preform impregnation, constant fiber volumetric fraction and less void content [49,50]. Heating slopes and curing steps are described in Figure 2b.

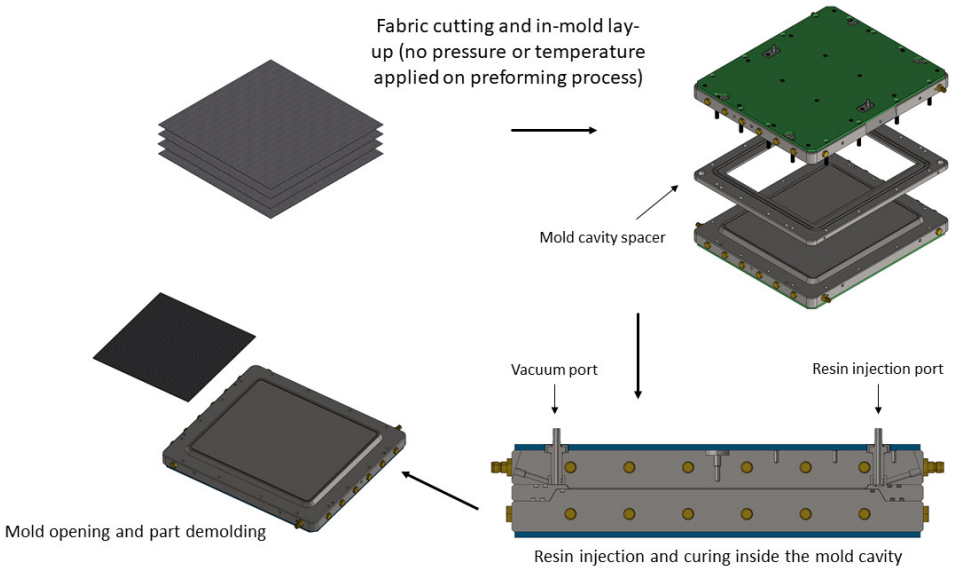

(**a**)

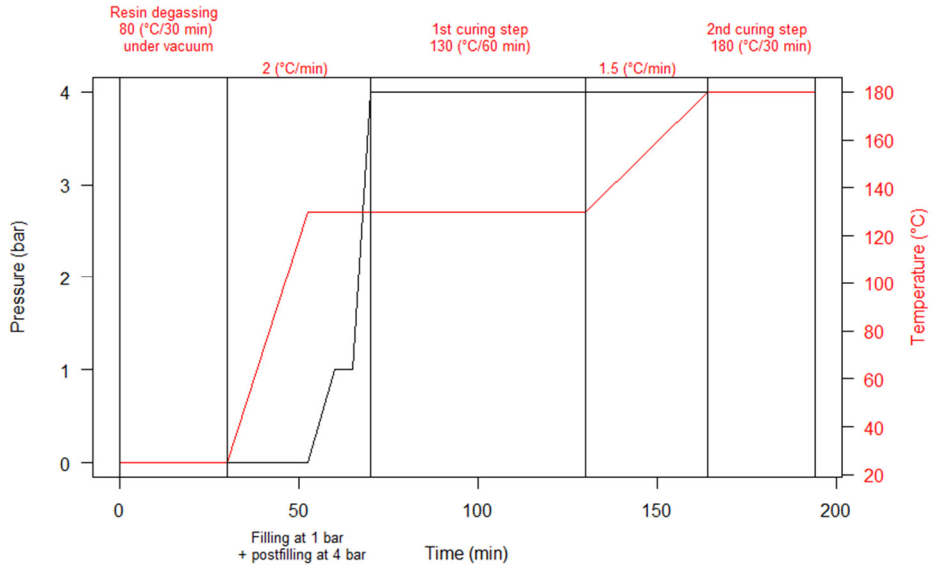

(**b**)

Figure 2. Detail of manufacturing procedure. (**a**) Process steps for composite manufacture. (**b**) Process conditions for injection and curing.

Samples were validated prior to machining through visual inspection and C-scans (Figure 3a,b), and cutting was done using a waterjet.

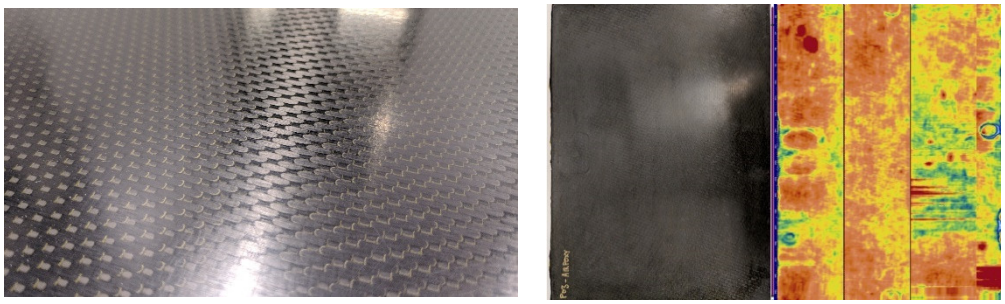

(**a**) (**b**)

Figure 3. Preparation of AIR-3R test samples. (**a**) Visual inspection of the carbon fiber sheet manufactured inside the RTM molds. (**b**) Ultrasonic C-Scan inspection of the manufactured carbon fiber sheets prior to samples cutting.

2.3. Tests and Equipments

Neat resin tensile tests were performed following the ISO 527-2:2012 standard [51] on five dumbbell-shaped specimens (type 1B) of 150 mm in total length, 20 mm in total width and a thickness of 4 mm. The testing area had a length of 50 mm and a width of 10 mm. Test was carried out at a speed of 1 mm/min.

Neat resin flexural tests were performed following the ISO 178:2019 standard [52] in a three-point test configuration. The specimen dimensions were 80 mm length, 10 mm width and 4 mm thickness. Five specimens were tested at a speed rate of 2 mm/min.

Composites tensile tests were performed following the ISO 527-4:1997 standard [53] on specimens of 250 mm × 25 mm with 2 mm thickness (tabbed type 3) for the 5HS fabric and 250 mm × 15 mm and 1 mm thickness for the UD. Five specimens were tested for each reinforcement. Tests were carried out at a speed of 2 mm/min. A biaxial extensometer was applied to obtain strain measurements.

Neat resin tensile and flexural test and composite tensile tests were carried out on an Instron 5985 universal testing machine (Barcelona, Spain).

Compression tests were performed following the ISO 14126:1999 standard for the 5HS fabric [54] at the speed of 0.5 mm/min. Ten 110 mm × 10 mm specimens with 2 mm thickness (tabbed type A) were tested. The UD tests were performed following the ASTM D3410/B standard [55] with specimen dimensions of 150 mm × 10 mm × 3 mm. Strain gages were applied on both sides of the specimens. An anti-buckling device was used following the requirements from the ASTM standard (ITTRI test fixture).

Interlaminar shear strength tests were performed following the ISO 14130:1997 standard [56] at a loading rate of 1mm/min. Specimen dimensions were 20 mm × 10 mm × 2 mm thickness.

In-plane shear tests were performed following the ISO 14129:1997 standard [57] with a loading rate of 2 mm/min. Specimen dimensions were 250 mm × 25 mm × 2 mm thickness (tabbed specimens). Deformations were measured using a biaxial extensometer.

Open-hole tension and compression tests were performed following ASTM standards D5766M [58] and ASTMD6484M [59], respectively. Specimens were 3 mm thick, 300 mm long and 36 mm wide. The hole diameter was 6 mm. Tests were carried out at speeds of 2mm/min (OHT) and 1mm/min (OHC).

Filled-hole compression tests were performed following the ASTM D6742M standard [60]. Specimen dimensions were 300 mm × 36 mm with 3 mm thickness and 6 mm hole diameter. The specimen was mounted with a titanium protruding-head HI-LOK DAN7-8-3 fuse pin (IDEC, Vitoria, Spain). Tests were carried out on five specimens at a speed of 1 mm/min. A specific support fixture was used to prevent the coupons buckling in the OHC and FHC tests.

Compression, ILSS, IPS, OHT, OHC and FHC tests were carried out on an MTS series 332.31 dynamic testing machine (SEM Engineering. Barcelona, Spain). Two different load cells were used: MTS 661.20F-02 50 kN load cell for the ILSS test and MTS 661.22D-01 250 kN for compression, IPS, OHT, OHC and FHC tests.

Mode I fracture toughness (G_{IC}) tests were performed following the EN 6033:2015 standard [61]. Sample dimensions were 250 mm × 25 mm × 3.2 mm thickness. Inside the specimens, 0.01 mm-thick PTFE release film was used to create a crack in the laminate. Tests were carried out on a ZwickRoell 3 testing machine at a speed of 10 mm/min. Test was applied in the interlaminar configuration.

Mode II fracture toughness (G_{IIC}) tests were performed following standard EN 6034:2015. [62]. The sample length was 115 mm long, 25 mm wide and 3 mm thick. Tests were carried out on a ZwickRoell 3 testing machine (Leominster, United Kingdom) at a speed of 1 mm/min. Test was applied in the interlaminar configuration.

The glass transition temperature was measured following the ISO 11357-2:2013 standard [63] through differential scanning calorimetry test (DSC). Samples were heated until 230 °C at a rate of 10 °C/min. Two heating steps were applied, and tests were carried out on a DSC Q20 TA Instruments machine (Cerdanyola del Vallès, Spain).

2.4. Baseline Properties

A set of baseline material properties relevant for aeronautical applications were defined in order to compare the AIR-3R resin behavior as a matrix for fiber-reinforced composites [47]. The objective of this vitrimer composite is to be mechanically comparable to and compete with the most widely used thermoset resin systems in the RTM process in the aeronautical industry, such as the HexFlow® RTM6 from Hexcel (Madrid, Spain) [64]. Baseline data was scaled up to 10% to account for the fact that the reference composite properties have been obtained with a standard modulus fiber, whereas in this work, we use an intermediate modulus fiber (around 20% difference in the respective tensile modulus [65–68]). All conventional thermoset values were collected with samples manufactured by RTM using the RTM6 resin (referred to as STD-AR from here on). Baseline values are summarized in Table 2.

3. Results and Discussion

3.1. T_g

The T_g of the AIR-3R vitrimer obtained by DSC was 170 °C ± 3 °C, which is equal to the baseline requirement. The DSC showed that the current curing process led to a degree of complete curing. AIR-3R had a lower T_g than the standard aeronautic thermoset references (Table 1) but was still much higher than most of the vitrimer formulations reported so far. The VA vitrimer from S. Wang et al. [23] shows almost the same T_g value due to the high rigidity of the Schiff-based structure, as the cross-linking density was proved to be low, and the vitrimer formulation made by Y. Yuan et al. [6] exhibited a higher T_g, being more equivalent to the aeronautic thermoset references, also due to the strong network structure, composed in this case by C-N covalent bonds.

We measured the water uptake of the AIR-3R vitrimer under 70 °C/85% RH, with a mass gain of 2.3% after 30 days until moisture equilibrium. The measured T_g after this was 155 °C, having a reduction of 8.8% of the pristine value, validating related findings on the effects of moisture on the glass transition temperature of epoxies [69,70]. The T_g value of the aged AIR-3R vitrimer is still above the highest temperature and humidity condition, meaning that it should not affect its final performance under these conditions.

3.2. Neat Vitrimer Tension

The AIR-3R neat vitrimer resin presented better tensile modulus and tensile strength (Figure 4) compared with the neat baseline properties, with improvements of 11.37% and 10.71%, respectively.

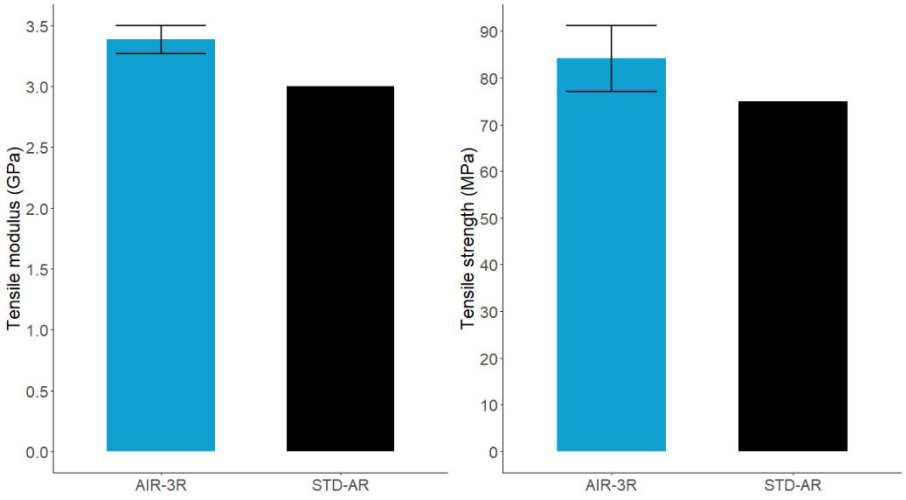

Figure 4. Tensile modulus (**left**) and strength (**right**) for the neat vitrimer and baseline reference.

3.3. Neat Vitrimer Flexion

The flexural modulus of the AIR-3R formulation was similar to the baseline, although the flexural strength was slightly lower, with a difference of −11.3%. It still had comparable mechanical behavior (Figure 5).

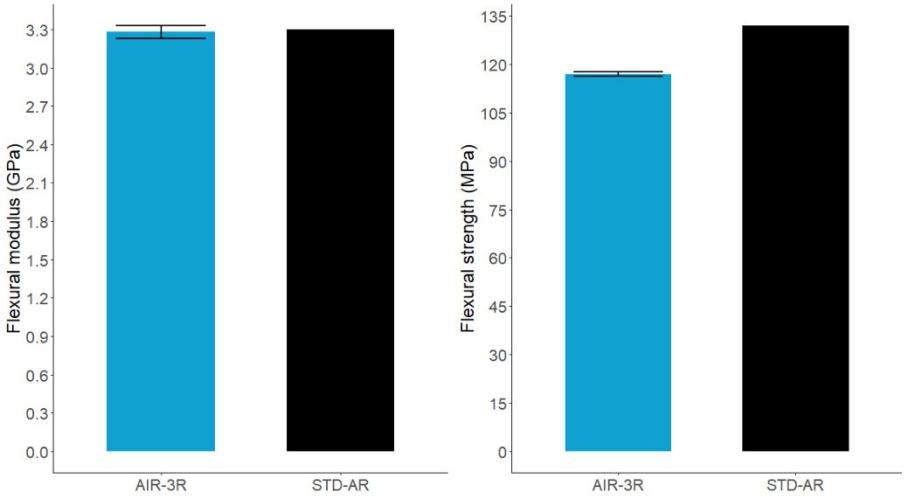

Figure 5. Flexural modulus (**left**) and strength (**right**) for the neat resin vitrimer and baseline reference.

Other reported vitrimer formulations have quite similar tensile properties, most being slightly under of this formulation [9,10,13,20,23,71]. Only the Imine–Amine-based vitrimer formulation from H. Liu et al. [2] and the 2,2-bis[4-(4-aminophenoxy)phenyl]propane formulation from Y. Yuan et al. [6] presented better tensile properties related to the high rigidity of their polymer networks, the latter also having better flexural properties. I. Aranberri et al. reported similar flexural properties on a DGEBA-disulfide vitrimer formulation [72]. The overall mechanical properties of the AIR-3R formulation are quite similar to the thermoset baseline, meaning that the use of this dynamic formulation would not affect the performance of structural components.

3.4. Tension

Figures 6 and 7 show a comparison of the tensile modulus and tensile strength for the reinforcements studied under the different test conditions. For cross-ply and UD 0° reinforcements, tensile modulus performed slightly better in the three different conditions than the defined properties based on the aeronautic thermoset baseline: 8.7% and 1.3% at RT, 7% and 1.9% at HW70 and 6.6% and 11.9% at HW120, respectively. The same tendency is observed for tensile strength, with increments of 8.2% for cross-ply and 5.4% for UD 0° at RT and 1.8% (cross-ply) and 5.8% (UD 0°) for HW70. In the highest-temperature condition (HW120), AIR-3R performed slightly worse: −2.9% (cross-ply) and −6.7% (UD 0°). The T_g of the AIR-3R after aging was already lower than the pristine value, being in this case closer to the HW120 condition and possibly reducing its performance. However, we consider that under tension, most of the load is sustained by the reinforcement rather than the matrix. These results demonstrate that this new vitrimeric formulation does not interfere with the composite's performance [9].

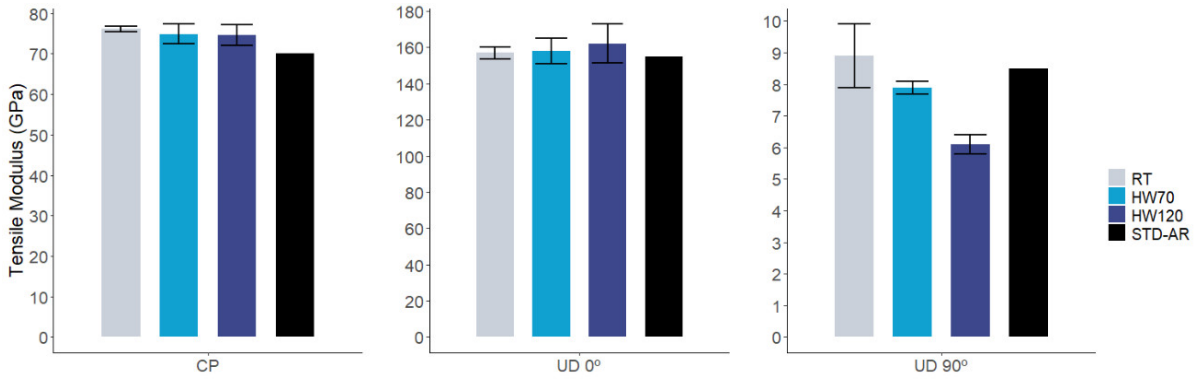

Figure 6. Comparative results in tensile modulus for AIR-3R vitrimer for different fabrics and test conditions. STD-AR composites tested under the three temperature and humidity conditions; one bar displayed as the final value was equivalent for the three cases (fiber dominant property).

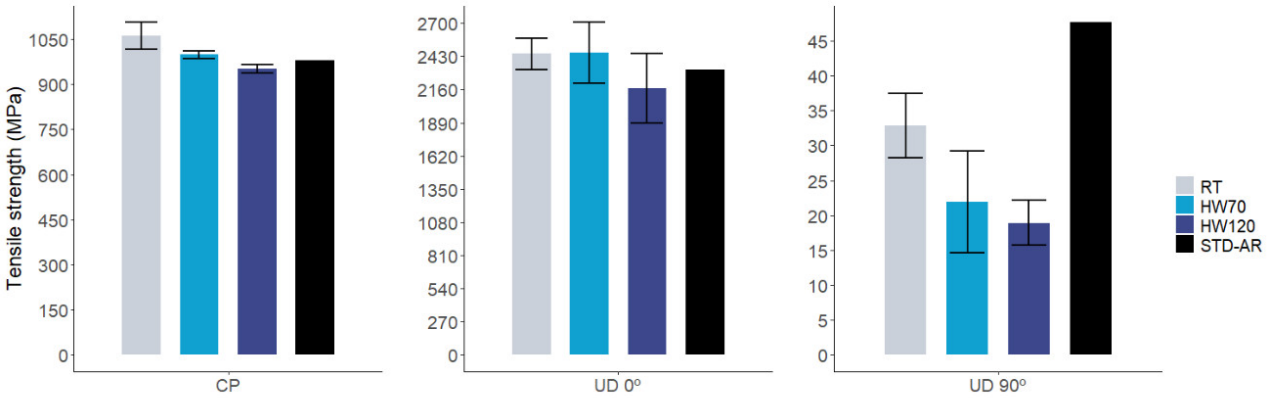

Figure 7. Comparative results in tensile strength for AIR-3R vitrimer for different fabrics and test conditions. STD-AR composites tested under the three temperature and humidity conditions; one bar displayed as the final value was equivalent for the three cases (fiber dominant property).

However, the UD 90° fabric's performance was different: the relative variation of the modulus was 4.7%, −7% and −28.2% for RT, HW70 and HW120 conditions, respectively. The tensile strength decreased by −31.1%, −54% and −60.3% at RT, HW70 and HW120, respectively. In this matrix-dominated load case, the drop in mechanical performance is important if compared with the defined baseline. H. Hamada et al. [73], and later R. Maurin et al. [74], reported that tensile properties on UD CF in 90° are complex to determine. Fiber presence acts as a stress concentrator inside the matrix, so the matrix is a dominant factor, but the strength also depends on the fibers' nature, chemistry and their interfacial properties and quality. Effects of the decreased T_g caused by the water uptake also have to be considered. Fracture analysis in the samples would be necessary in order to understand the dominant effect on the AIR-3R transverse tensile properties.

3.5. Compression

Compression test results present a high variability, inherent to the test setup. About 50% of the samples tested had to be discarded because of invalid failure modes. A percent bending strain (PBS) threshold of 10% was established for the test to be considered valid. Above this value, the coupon experiences non-neglectable load models such as bending, buckling or torsion.

Compression modulus (Figure 8) of cross-ply fabric composites with AIR-3R vitrimer was higher than the defined baseline by 8.8% in RT and HW70 and 11.9% in HW120. For the UD 0° composite with the vitrimer, the compression modulus was within 1% above

the reference. In the UD 90° fabric, at RT, AIR-3R overpassed the thermoset formulation, but under high temperature and humidity, it presented a slightly inferior response, albeit still comparable with the thermoset counterpart: 22.2% in RT, −3.5% in HW70 and −5.9% in HW120.

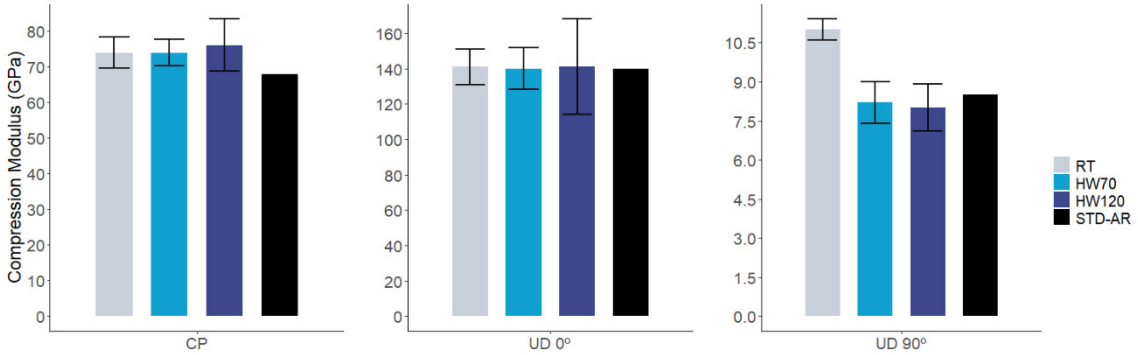

Figure 8. Comparative results in compression modulus for AIR-3R vitrimer for different fabrics and test conditions. STD-AR composites tested under the three temperature and humidity conditions; one bar displayed as the final value was equivalent for the three cases (fiber dominant property).

Compression strength (Figure 9) of the vitrimer composites presented an abrupt drop in most of the conditions: −24.8% in RT, −26.3% in HW70 and 25.6% in HW120 for the cross-ply fabric; −40.6% in RT, −44.9% in HW70 and −35.3% in HW120 for UD 0°; and −24.2% in RT, −39.3% in HW70 and −11.8% in HW120 for UD 90°.

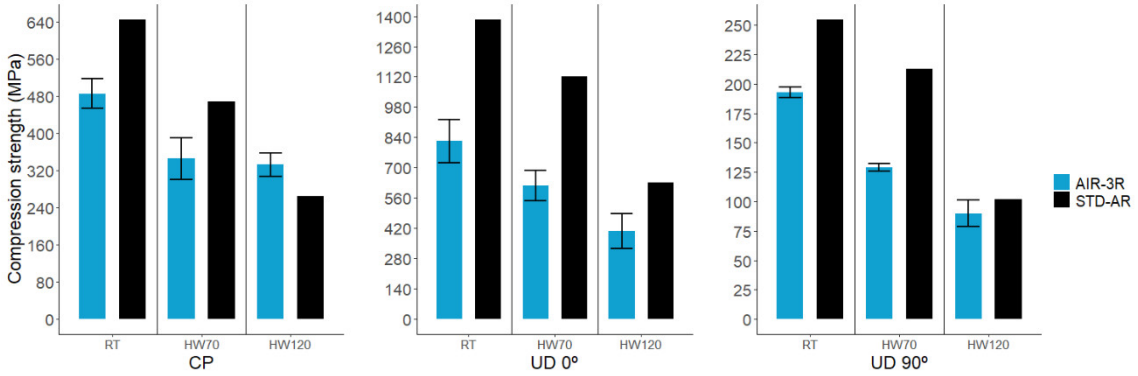

Figure 9. Comparative results in compression strength for AIR-3R vitrimer for different fabrics and test conditions. Samples with the PA veil.

To better understand this compressive strength behavior, we took micrography images (Figure 10) of the AIR-3R samples. Some gray-rounded areas appear between the fiber layers corresponding to the thermoplastic PA veil initially included in the carbon fiber fabrics. According to the manufacturer, this veil has a melting temperature close to 180 °C that corresponds to the in-mold post-curing temperature of the AIR-3R vitrimer formulation. In the first curing step (130 °C), the vitrimer starts to polymerize, embedding the veil structure inside the laminate. Therefore, even if this veil later melts, it is trapped by the already frozen structure of the vitrimer matrix, possibly acting as a contaminant or stress concentrator.

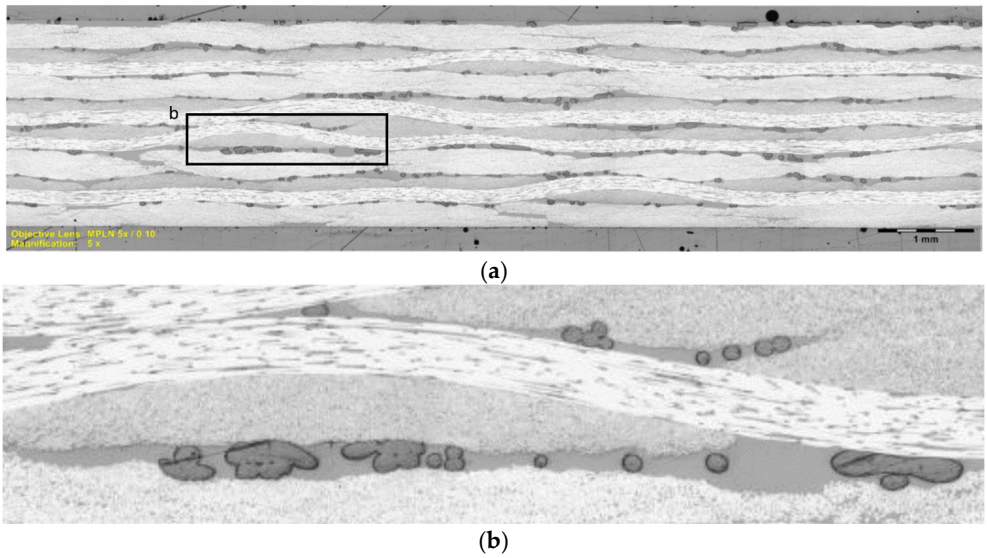

Figure 10. Micrography images of AIR-3R composite sample. (**a**) Panel cross-section. (**b**) Detail of layers interface in the laminate. Objective lens MPLN 5X/0.10.

The PA veil was included in the AIR-3R vitrimer composite in order to enhance the interlaminar toughness and impact resistance, as has been demonstrated in several studies addressing interleaving thermoplastic veils [75–84]. In view of this microstructure, a new batch of tests was performed on samples without the thermoplastic PA veil; i.e., it was removed and all other conditions were maintained. The AIR-3R vitrimer performed comparably to the thermoset baseline reference with a slight difference of −2.8% in the compression strength. The presence of the PA veil caused a decrement in the compressive response of the vitrimer composite (Figure 11). Related publications detail that thermoplastic veils acting as interleaves often increase the fracture toughness by serving as an obstacle to crack propagation but, as a countereffect, lowering the composite's in-plane properties. Thermoplastic veils that do not melt during the manufacturing process have more permeability than the fibers, thus creating resin-rich zones and promoting voids. The higher the veil's aerial weight, the more the detrimental effect on the mechanical response is accentuated [77,78,80,85–87]. One of these studies reports that with a 4 g/m^2 co-PA veil, the compression strength decreases by 9%. In this work, the PA veil had double the aerial weight, which negatively impacted the compression strength by 22.6%.

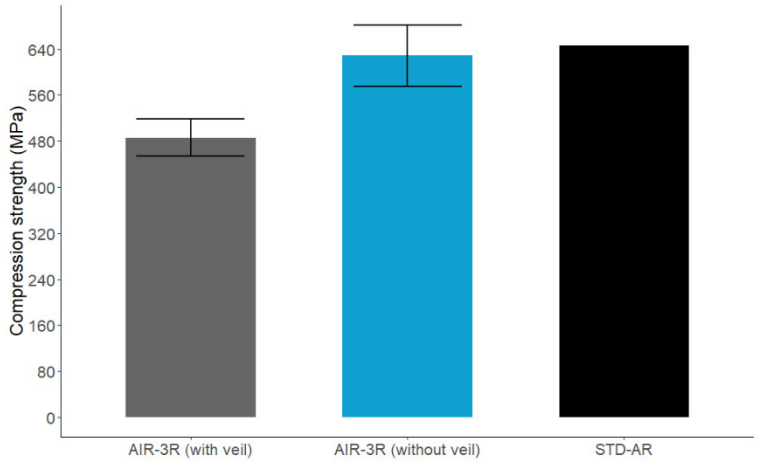

Figure 11. Comparison of the compressive strength for the AIR-3R vitrimer with and without the PA veil and the base thermoset reference. Cross-ply fabric tested under RT condition.

In view of the results with and without veil, it is concluded that the AIR-3R vitrimer formulation has no detrimental effect on the compressive strength of the final composite, thus being mechanically comparable to the thermoset baseline resin.

When comparing it to the vitrimers reported in the literature, AIR-3R has a superior compressive strength in reference to the 2,2-bis[4-(4-aminophenoxy)phenyl]propane-based formulation from Y. Yuan et al. [6]. In this point, we have to highlight that their neat vitrimer properties were higher that the AIR-3R formulation. The difference could be related to the lower fiber content in their composites (50.1% for a plane-weave fabric in a cross-ply configuration). It is also superior in compressive strength to the vitrimer from A. Ruiz de Luzuriaga et al. [9], which has a glass fiber reinforcement instead of carbon fiber.

3.6. Interlaminar Shear Strength

In all temperature conditions, the AIR-3R vitrimer performed well (Figure 12). The cross-ply fabric response was comparable to the baseline thermoset. Only at RT did it slightly underperform: −10% in RT, 7.1% in HW70 and 0% in HW120. For the UD, shear performance was superior to the baseline, even reaching an outstanding performance at the higher temperature condition: 20% in RT, 40% in HW70 and 43.3% in HW120.

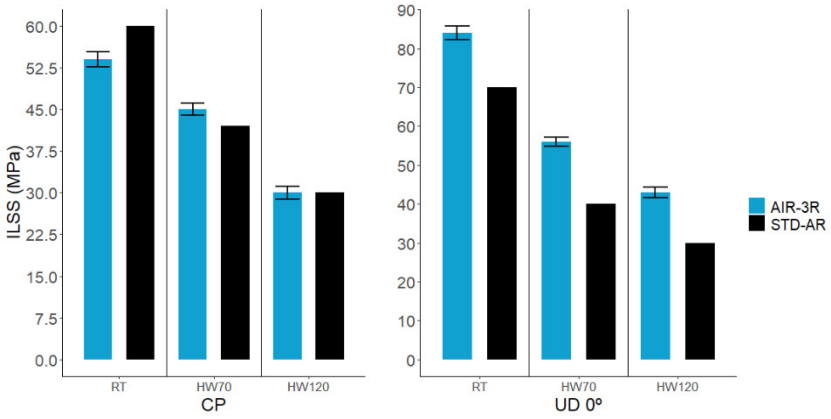

Figure 12. ILSS shear performance of the AIR-3R vitrimer formulation for different fabrics and test conditions.

In view of the influence of the PA veil on the compression response, another batch of ILSS samples was manufactured with the cross-ply fabric without the PA veil and tested at RT. These samples showed better performance than the original testing set, surpassing the baseline thermoset by 20% (Figure 13) and demonstrating than the presence of the PA veil in the laminate causes a 24.89% loss in the interlaminar shear performance.

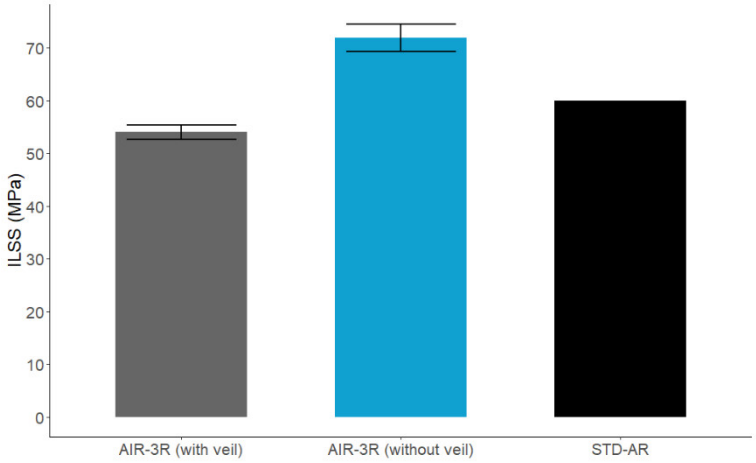

Figure 13. Comparison of the interlaminar shear strength for the AIR-3R vitrimer with and without the PA veil and base thermoset reference. Cross-ply fabric tested under RT condition.

3.7. In-Plane Shear

The IPS modulus for the vitrimer composite was generally better than the thermoset-based composite in both cross-ply and UD fabrics, particularly in high-temperature conditions (Figure 14): −2.2% in RT, 5.5% in HW70 and 17.4% in HW120 for CP fabric, and 2.3% in RT, 8.6% in HW70 and 22.7% in HW120 for UD.

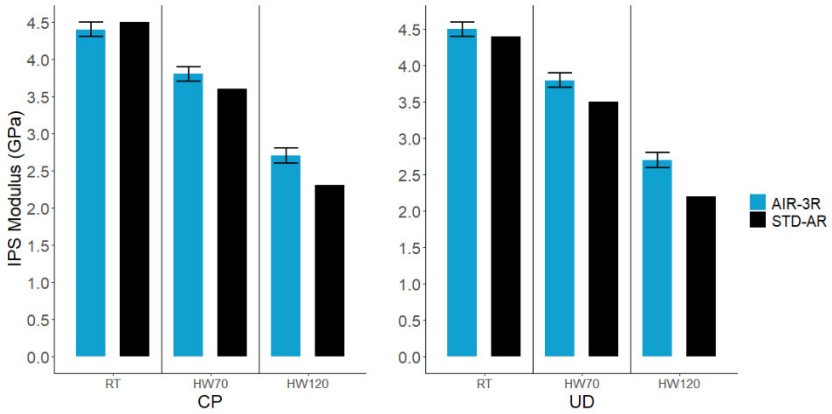

Figure 14. In-plane shear modulus of the AIR-3R vitrimer formulation for different fabrics and test conditions.

Regarding the in-plane shear strength (Figure 15), the vitrimer composite underperformed the baseline: −10% in RT, −17.7% in HW70 and −21.5% in HW120 for the cross-ply fabric, and −17.1% in RT, −11.5% in HW70 and −10.5% in HW120 for the UD.

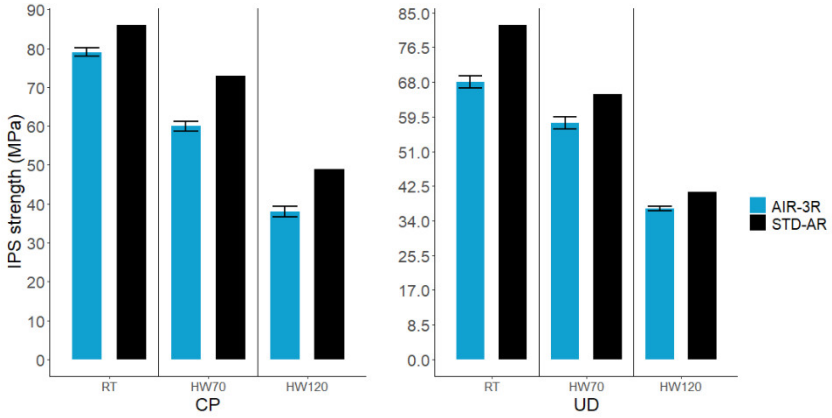

Figure 15. In-plane shear strength of the AIR-3R vitrimer formulation for different fabrics and test conditions.

The ILSS shear strength and IPS shear modulus suggest that the AIR-3R vitrimer has good toughness, good adhesion to the reinforcements, good adhesion between layers and good shear resistance, even after hot wet conditioning of the specimens. As was seen for the ILLS, the lower in-plane shear strength could be attributed to the thermoplastic PA veil inside the laminate.

AIR-3R ILSS performance was slightly higher compared with other vitrimer formulations, being comparable with the Imine VA/HTDA system [20]. The BAPP vitrimer system [6] has better shear performance, due to the network structure. The Vurea–Amine vitrimers [25,26] had comparable IPS shear modulus (4.7 GPa) to the AIR-3R vitrimer composite but lower shear strength (41 MPa).

3.8. Open-Hole Tension, Compression and Filled-Hole Compression

3.8.1. Open-Hole Tension

At RT conditions, the AIR-3R formulation is comparable to the base thermoset resin (Figure 16). After moisture saturation, testing at 70 °C presented a superior strength: 4.5% and 29.8%, respectively. All specimens presented good failure modes (Figure 17). Again, fibers carry most of the load, indicating no alternations in composite behavior.

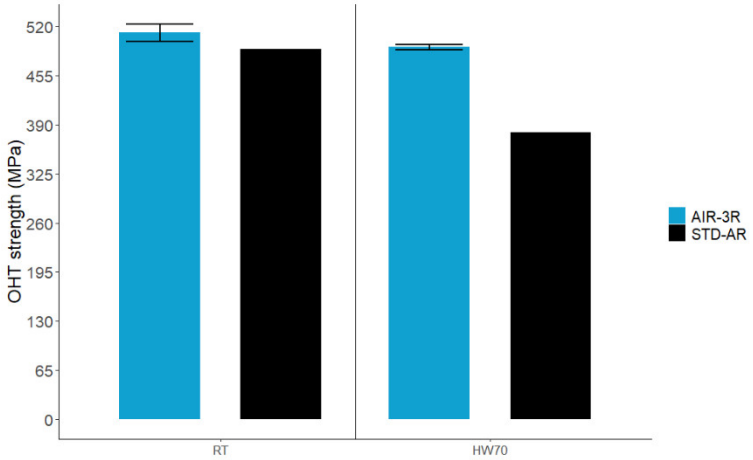

Figure 16. OHT test for the AIR-3R vitrimer composite under test conditions.

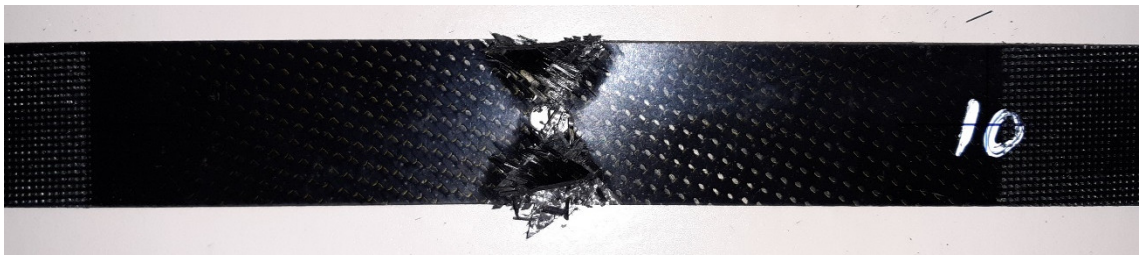

Figure 17. AIR-3R failed specimen under OHT test.

3.8.2. Open-Hole Compression

Specimens had a proper failure mode under the specified standard. The AIR-3R vitrimer had a slightly lower compressive strength than the thermoset baseline (Figure 18). The PA veil is likely behind these results, considering the effect on the compression and shear tests.

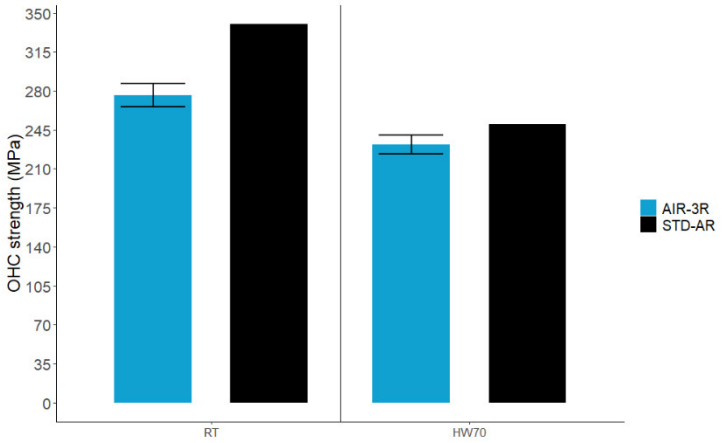

Figure 18. OHC test for the AIR-3R vitrimer composite under test conditions.

3.8.3. Filled-Hole Compression

The FHC strength for the AIR-3R vitrimer composite was slightly lower (−13.6%) than the baseline at RT and reached the same value for the HW70 condition (Figure 19). All the specimens presented non-valid failure modes, as they failed outside the bolt area. The attempts to improve this issue by tightening the jig bolts and by ensuring a correct alignment of the sample and parallelism of the loading plates did not succeed.

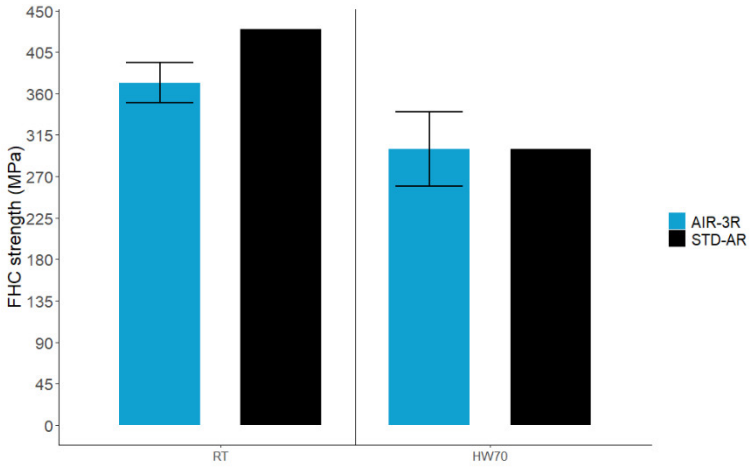

Figure 19. FHC test for the AIR-3R vitrimer composite under test conditions.

Nevertheless, the results are still comparable to the base thermoset composite. There are no reports of other vitrimer formulations having been tested on OHT, OHC and FHC.

3.9. Interlaminar Fracture Toughness

The AIR-3R vitrimer specimens presented lower fracture toughness under mode I (G_{IC}) at RT but were still comparable to the base thermoset resin in that they exhibited a 11.4% difference (Figure 20).

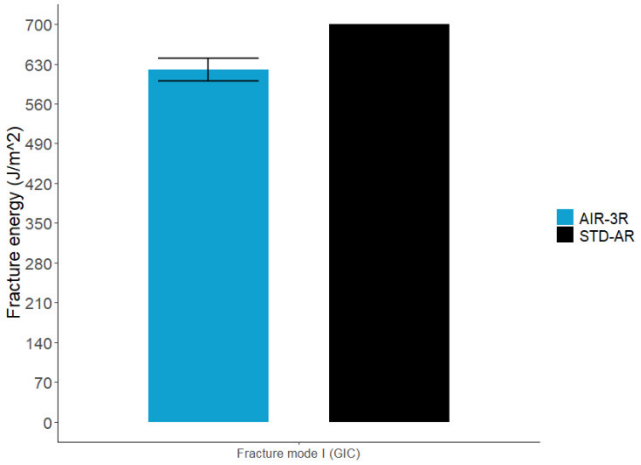

Figure 20. Fracture toughness for AIR-3R vitrimer composite.

A baseline value for the fracture toughness under mode II (G_{IIC}) was not defined. The AIR-3R vitrimer composite presented a mean energy value of 876.19 J/m².

Fracture toughness under mode I (G_{IC}) was comparable to reported thermoset composites toughened with thermoplastic veils: T300 UD CF 167 g/m²–Epoxy RTM6-2 with 20 wt% PAEK veil [88], UD CF 350 g/m²–Epoxy L160 with 17 g/m² PA-66 veil [75], Epoxy MTM57/T700S (24K) UD prepreg with 4.5 g/m² and 9 g/m² PA-66 veils [89]. Despite the differences in the veil materials, toughening mechanisms and mechanical responses were similar. Factors such as veil polymer type and aerial weight were more important in the performance of the final laminate.

Mode II (G_{IIC}) fracture toughness was lower than in similar thermoset composites toughened with thermoplastic veils. [79,88–90]. Toughening mechanisms in mode II (G_{IIC}) were more complex than mode I (G_{IC}), depending on most on the neat properties of the matrix and the architecture of the reinforcement, rather than the fiber bridging effect. The clarification of this topic deserves further research.

4. Conclusions and Outlook

The neat vitrimer properties demonstrate that this formulation can be used as a matrix for high-performance structural components, having similar properties to the thermoset baseline and thus not affecting their performance. This new epoxy–disulfide vitrimer composite has good in-plane stiffness under tension and compression and good shear stiffness, denoting good adhesion between fibers at the interface. Vitrimer composite strength under compression and interlaminar shear was proven to be highly influenced by the presence of the un-melted thermoplastic veil, which had been intended to enhance the fracture toughness. Micrography analysis and comparison to related studies show that the un-melted veil creates brittle resin-rich zones. Compression samples without the PA veil demonstrated that this trapped interface in the laminate reduces the compressive strength by 22.6%, while the ILSS samples presented reductions of 24.89%. The interlaminar veils could also have influenced the tension strength at UD 90°, in-plane shear

strength, OHC and FHC strength, all of which were lower than the base thermoset formulation.

Fracture toughness in mode I (G_{IC}) was comparable to reported thermoset formulations with toughening thermoplastic veils. Mode II appears to be lower than the references with and without the thermoplastic veils. Further research should be carried out to clarify the micro-mechanisms behind the fracture behavior of this vitrimer formulation, as well as the impact of the thermoplastic veils, their melting temperature and aerial weight on the in-plane vitrimer composite properties.

In summary, the mechanical properties of the AIR-3R and the composites prepared with this new vitrimer formulation were comparable to those currently used in aircraft materials. Dynamic properties of this particular formulation have to be studied in order to establish a processing window in which this formulation could be reprocessed by maintaining the overall composite properties.

Autor contributions: Formal analysis, V.G.; Investigation, V.G. and P.D.K.; Methodology, V.G.; Project administration, M.E.R.; Resources, A.M.S., A.R.d.L., N.M. and D.C.Z.; Validation, A.M.S., A.R.d.L. and N.M.; Visualization, C.B.C.; Writing—original draft, C.B.C.; Writing—review and editing, J.C. All authors have read and agreed to the published version of the manuscript.

Funding: This work was financially supported by the EU Horizon 2020 research and innovation project AIRPOXY with grant agreement 769274 under the H2020-MG-2017-Two-Stage call. J. Costa acknowledges the support of the Spanish MICINN, through the project RTI2018-097880-B-I00.

Institutional Review Board Statement: Not applicable.

Informed Consent Statement: Not applicable.

Data Availability Statement: Not applicable.

Acknowledgments: Special thanks to Núria Latorre Lázaro for her support.

Conflicts of interest: The authors declare there are no conflicts of interest to disclose.

References

1. Yang, Y.; Xu, Y.; Ji, Y.; Wei, Y. Functional epoxy vitrimers and composites. *Prog. Mater. Sci.* **2021**, *120*, 100710, https://doi.org/10.1016/j.pmatsci.2020.100710.
2. Liu, H.; Zhang, H.; Wang, H.; Huang, X.; Huang, G.; Wu, J. Weldable, malleable and programmable epoxy vitrimers with high mechanical properties and water insensitivity. *Chem. Eng. J.* **2019**, *368*, 61–70, https://doi.org/10.1016/j.cej.2019.02.177.
3. Denissen, W.; Winne, J.M.; Du Prez, F.E. Vitrimers: Permanent organic networks with glass-like fluidity. *Chem. Sci.* **2016**, *7*, 30–38, https://doi.org/10.1039/c5sc02223a.
4. Dorigato, A. Recycling of thermosetting composites for wind blade application. *Adv. Ind. Eng. Polym. Res.* **2021**, *4*, 116–132, https://doi.org/10.1016/j.aiepr.2021.02.002.
5. Witik, R.A.; Teuscher, R.; Michaud, V.; Ludwig, C.; Månson, J.-A.E. Carbon fibre reinforced composite waste: An environmental assessment of recycling, energy recovery and landfilling. *Compos. Part A Appl. Sci. Manuf.* **2013**, *49*, 89–99, https://doi.org/10.1016/j.compositesa.2013.02.009.
6. Yuan, Y.; Sun, Y.; Yan, S.; Zhao, J.; Liu, S.; Zhang, M.; Zheng, X.; Jia, L. Multiply fully recyclable carbon fibre reinforced heat-resistant covalent thermosetting advanced composites. *Nat. Commun.* **2017**, *8*, 14657, https://doi.org/10.1038/ncomms14657.
7. Azcune, I.; Odriozola, I. Aromatic disulfide crosslinks in polymer systems: Self-healing, reprocessability, recyclability and more. *Eur. Polym. J.* **2016**, *84*, 147–160, https://doi.org/10.1016/j.eurpolymj.2016.09.023.
8. Montarnal, D.; Capelot, M.; Tournilhac, F.; Leibler, L. Silica-Like Malleable Materials from Permanent Organic Networks. *Science* **2011**, *334*, 965–968, https://doi.org/10.1126/science.1212648.
9. Ruiz de Luzuriaga, A.; Martin, R.; Markaide, N.; Rekondo, A.; Cabañero, G.; Rodríguez, J.; Odriozola, I. Epoxy resin with exchangeable disulfide crosslinks to obtain reprocessable, repairable and recyclable fiber-reinforced thermoset composites. *Mater. Horiz.* **2016**, *3*, 241–247, https://doi.org/10.1039/c6mh00029k.
10. Si, H.; Zhou, L.; Wu, Y.; Song, L.; Kang, M.; Zhao, X.; Chen, M. Rapidly reprocessable, degradable epoxy vitrimer and recyclable carbon fiber reinforced thermoset composites relied on high contents of exchangeable aromatic disulfide crosslinks. *Compos. Part B Eng.* **2020**, *199*, 108278, https://doi.org/10.1016/j.compositesb.2020.108278.
11. Kissounko, D.A.; Taynton, P.; Kaffer, C. New material: Vitrimers promise to impact composites. *Reinf. Plast.* **2018**, *62*, 162–166, https://doi.org/10.1016/j.repl.2017.06.084.
12. Yang, Y.; Peng, G.; Wu, S.; Hao, W. A repairable anhydride-epoxy system with high mechanical properties inspired by vitrimers. *Polym.* **2018**, *159*, 162–168, https://doi.org/10.1016/j.polymer.2018.11.031.

13. Yu, Q.; Peng, X.; Wang, Y.; Geng, H.; Xu, A.; Zhang, X.; Xu, W.; Ye, D. Vanillin-based degradable epoxy vitrimers: Reprocessability and mechanical properties study. *Eur. Polym. J.* **2019**, *117*, pp. 55–63, https://doi.org/10.1016/j.eurpolymj.2019.04.053.
14. Ji, F.; Liu, X.; Sheng, D.; Yang, Y. Epoxy-vitrimer composites based on exchangeable aromatic disulfide bonds: Reprocessibility, adhesive, multi-shape memory effect. *Polymers* **2020**, *197*, 122514, https://doi.org/10.1016/j.polymer.2020.122514.
15. Feng, X.; Li, G. Catalyst-free β-hydroxy phosphate ester exchange for robust fire-proof vitrimers. *Chem. Eng. J.* **2021**, *417*, 129132, https://doi.org/10.1016/j.cej.2021.129132.
16. Krishnakumar, B.; Sanka, R.V.S.P.; Binder, W.H.; Park, C.; Jung, J.; Parthasarthy, V.; Rana, S.; Yun, G.J. Catalyst free self-healable vitrimer/graphene oxide nanocomposites. *Compos. Part B Eng.* **2020**, *184*, 107647, https://doi.org/10.1016/j.compositesb.2019.107647.
17. Han, J.; Liu, T.; Hao, C.; Zhang, S.; Guo, B.; Zhang, J. A Catalyst-Free Epoxy Vitrimer System Based on Multifunctional Hyperbranched Polymer. *Macromolecules* **2018**, *51*, 6789–6799, https://doi.org/10.1021/acs.macromol.8b01424.
18. Zhao, W.; An, L.; Wang, S. Recyclable High-Performance Epoxy-Anhydride Resins with DMP-30 as the Catalyst of Transesterification Reactions. *Polymers* **2021**, *13*, 296, https://doi.org/10.3390/polym13020296.
19. Liu, Y.; Wang, B.; Ma, S.; Yu, T.; Xu, X.; Li, Q.; Wang, S.; Han, Y.; Yu, Z.; Zhu, J. Catalyst-free malleable, degradable, bio-based epoxy thermosets and its application in recyclable carbon fiber composites. *Compos. Part B Eng.* **2021**, *211*, 108654, https://doi.org/10.1016/j.compositesb.2021.108654.
20. Memon, H.; Wei, Y.; Zhang, L.; Jiang, Q.; Liu, W. An imine-containing epoxy vitrimer with versatile recyclability and its application in fully recyclable carbon fiber reinforced composites. *Compos. Sci. Technol.* **2020**, *199*, 108314, https://doi.org/10.1016/j.compscitech.2020.108314.
21. Zhu, Y.; Gao, F.; Zhong, J.; Shen, L.; Lin, Y. Renewable castor oil and DL-limonene derived fully bio-based vinylogous urethane vitrimers. *Eur. Polym. J.* **2020**, *135*, 109865, https://doi.org/10.1016/j.eurpolymj.2020.109865.
22. Alabiso, W.; Schlögl, S. The Impact of Vitrimers on the Industry of the Future: Chemistry, Properties and Sustainable Forward-Looking Applications. *Polymer* **2020**, *12*, 1660, https://doi.org/10.3390/polym12081660.
23. Wang, S.; Ma, S.; Li, Q.; Xu, X.; Wang, B.; Yuan, W.; Zhou, S.; You, S.; Zhu, J. Facile in situ preparation of high-performance epoxy vitrimer from renewable resources and its application in nondestructive recyclable carbon fiber composite. *Green Chem.* **2019**, *21*, 1484–1497, https://doi.org/10.1039/c8gc03477j.
24. Chabert, E.; Vial, J.; Cauchois, J.-P.; Mihaluta, M.; Tournilhac, F. Multiple welding of long fiber epoxy vitrimer composites. *Soft Matter* **2016**, *12*, 4838–4845, https://doi.org/10.1039/c6sm00257a.
25. Denissen, W.; De Baere, I.; Van Paepegem, W.; Leibler, L.; Winne, J.; Du Prez, F.E. Vinylogous Urea Vitrimers and Their Application in Fiber Reinforced Composites. *Macromolecules* **2018**, *51*, 2054–2064, https://doi.org/10.1021/acs.macromol.7b02407.
26. De Baere, I.; Denissen, W.; Van Paepegem, W.; Winne, J.; Du Prez, F. Assessement of urea based vitrimers as a new matrix material for fibre reinforced polymers. In Proceedings of the ECCM18—18th European Conference on Composite, Athens, Greece, 24–28 June 2018. Available online: http://hdl.handle.net/1854/LU-8569138 (accessed on 16 September 2021).
27. Bangash, M.K.; Ruiz de Luzuriaga, A.; Aurrekoetxea, J.; Markaide, N.; Grande, H.-J.; Ferraris, M. Development and characterisation of dynamic bi-phase (epoxy/PU) composites for enhanced impact resistance. *Compos. Part B Eng.* **2018**, *155*, 122–131, https://doi.org/10.1016/j.compositesb.2018.08.039.
28. Taynton, P.; Ni, H.; Zhu, C.; Yu, K.; Loob, S.; Jin, Y.; Qi, H.J.; Zhang, W. Repairable Woven Carbon Fiber Composites with Full Recyclability Enabled by Malleable Polyimine Networks. *Adv. Mater.* **2016**, *28*, 2904–2909, https://doi.org/10.1002/adma.201505245.
29. MALLINDA. Vitrimer Matrix Composites for the Circular Economy. Available online: https://www.mallinda.com/ (accessed on 9 September 2021).
30. Taynton, P.; Yu, K.; Shoemaker, R.; Jin, Y.; Qi, H.J.; Zhang, W. Heat- or Water-Driven Malleability in a Highly Recyclable Covalent Network Polymer. *Adv. Mater.* **2014**, *26*, 3938–3942, https://doi.org/10.1002/adma.201400317.
31. Wang, S.; Xing, X.; Zhang, X.; Wang, X.; Jing, X. Room-temperature fully recyclable carbon fibre reinforced phenolic composites through dynamic covalent boronic ester bonds. *J. Mater. Chem. A* **2018**, *6*, 10868–10878, https://doi.org/10.1039/c8ta01801d.
32. Liu, X.; Li, Y.; Xing, X.; Zhang, G.; Jing, X. Fully recyclable and high performance phenolic resin based on dynamic urethane bonds and its application in self-repairable composites. *Polymers* **2021**, *229*, 124022, https://doi.org/10.1016/j.polymer.2021.124022.
33. Liu, T.; Hao, C.; Shao, L.; Kuang, W.; Cosimbescu, L.; Simmons, K.L.; Zhang, J. Carbon Fiber Reinforced Epoxy Vitrimer: Robust Mechanical Performance and Facile Hydrothermal Decomposition in Pure Water. *Macromol. Rapid Commun.* **2021**, *42*, e2000458, https://doi.org/10.1002/marc.202000458.
34. Wang, H.; Liu, H.-C.; Zhang, Y.; Xu, H.; Jin, B.-Q.; Cao, Z.-X.; Wu, H.-T.; Huang, G.-S.; Wu, J.-R. A Triple Crosslinking Design toward Epoxy Vitrimers and Carbon Fiber Composites of High Performance and Multi-shape Memory. *Chin. J. Polym. Sci.* **2021**, 1–9, https://doi.org/10.1007/s10118-021-2538-7.
35. Liu, Y.-Y.; He, J.; Li, Y.-D.; Zhao, X.-L.; Zeng, J.-B. Biobased epoxy vitrimer from epoxidized soybean oil for reprocessable and recyclable carbon fiber reinforced composite. *Compos. Commun.* **2020**, *22*, 100445, https://doi.org/10.1016/j.coco.2020.100445.
36. Liu, Y.-Y.; Liu, G.-L.; Li, Y.-D.; Weng, Y.; Zeng, J.-B. Biobased High-Performance Epoxy Vitrimer with UV Shielding for Recyclable Carbon Fiber Reinforced Composites. *ACS Sustain. Chem. Eng.* **2021**, *9*, 4638–4647, https://doi.org/10.1021/acssuschemeng.1c00231.

37. Xu, Y.; Dai, S.; Bi, L.; Jiang, J.; Zhang, H.; Chen, Y. Catalyst-free self-healing bio-based vitrimer for a recyclable, reprocessable, and self-adhered carbon fiber reinforced composite. *Chem. Eng. J.* **2021**, *429*, 132518, https://doi.org/10.1016/j.cej.2021.132518.
38. Hexcel Corporation. HexPly® 8552. 2020. Available online: https://www.hexcel.com/user_area/content_media/raw/ (accessed on 7 September 2021).
39. Hexion. EPIKOTE™ Resin 475 and EPIKURE™ Curing Agent 375 and HELOXY™ Additive 575. 2021. Available online: https://www.hexion.com/CustomServices/PDFDownloader.aspx?type=tds&pid=77f8c63d-5814-6fe3-ae8a-ff0300fcd525 (accessed on 7 September 2021).
40. Beier, U.; Fischer, F.; Sandler, J.K.; Altstädt, V.; Weimer, C.; Buchs, W. Mechanical performance of carbon fibre-reinforced composites based on stitched preforms. *Compos. Part A Appl. Sci. Manuf.* **2007**, *38*, 1655–1663, https://doi.org/10.1016/j.compositesa.2007.02.007.
41. AIRPOXY. Thermoformable, Repairable & Bondable Smart Epoxy-Based Composites for Aero Structures. Available online: https://www.airpoxy.eu/ (accessed on 7 July 2021).
42. European Commision. Thermoformable, Repairable and Bondable Smart Epoxy Based Composites for Aero Structures. 2018. Available online: https://cordis.europa.eu/project/id/769274 (accessed on 7 July 2021).
43. Odriozola, I.; Ruiz de Luzuriaga, A.; Rekondo, A.; Martin, R.; Markaide, N.; Cabañero, G.; Grande, H.J. Thermomechanically Reprocessable Epoxy Composites and Processes for Their Manufacturing. US20170166717A1, 3 December 2015.
44. Odriozola, I.; Ruiz de Luzuriaga, A.; Rekondo, A.; Martin, R.; Markaide, N.; Cabañero, G.; Grande, H.J. Composites de Epoxi Reprocesables Termomecánicamente y Procedimientos para su Fabricación. ES2682954T3, 24 September 2018.
45. Cidetec. 3R Leading Technology Reprocessable, Repairable and Recyclable: Materials with an Endless Lifespan. Available online: https://www.cidetec.es/en/top-achievements/3r-leading-technology (accessed on 7 July 2021).
46. Chomarat. C-WEAVE™ 280SA5 T800HB 6K. Available online: https://composites.chomarat.com/en/product/c-weave-280sa5-t800hb-6k/ (accessed on 7 July 2021).
47. De Fontgallant, A.; Calderón, D. AIRPOXY Deliverable 1.3: Report on the Preliminary Analysis and Definition of Specifications for the Raw Materials. 2019. Available online: https://www.airpoxy.eu/wp-content/uploads/AIRPOXY-D1.3-Preliminary-specifications-for-the-raw-materials_R1.0.pdf (accessed on 7 July 2021).
48. Calderón, D.; González, R.; De Fontgallant, A. AIRPOXY Deliverable 1.1: Report on the Preliminary Specifications for Demonstrators. 2019. Available online: https://www.airpoxy.eu/wp-content/uploads/AIRPOXY-D1.1-Preliminary-specifications-for-demonstrators_R1.0.pdf (accessed on 7 July 2021).
49. Simacek, P.; Eksik, Ömer; Heider, D.; Gillespie, J.W.; Advani, S. Experimental validation of post-filling flow in vacuum assisted resin transfer molding processes. *Compos. Part A Appl. Sci. Manuf.* **2012**, *43*, 370–380, https://doi.org/10.1016/j.compositesa.2011.10.002.
50. Olivero, K.A.; Barraza, H.J.; O'Rear, E.A.; Altan, M.C. Effect of Injection Rate and Post-Fill Cure Pressure on Properties of Resin Transfer Molded Disks. *J. Compos. Mater.* **2002**, *36*, 2011–2028, https://doi.org/10.1177/0021998302036016244.
51. ISO Standard. *Plastics—Determination of Tensile Properties—Part 2: Test Conditions for Moulding and Extrusion Plastics*; ISO 527-2:2012; International Organization for Standardization: Geneva, Switzerland, 2012.
52. ISO Standard. *Plastics—Determination of Flexural Properties*; ISO 178:2019; International Organization for Standardization: Geneva, Switzerland, 2019.
53. ISO Standard. Plastics—Determination of Tensile Properties—Part 4: Test Conditions for Isotropic and Orthotropic Fibre-Reinforced Plastic Composites; ISO 527-4:1997; International Organization for Standardization: Geneva, Switzerland, 1997.
54. ISO Standard. *Fibre-Reinforced Plastic Composites—Determination of Compressive Properties in the In-Plane Direction*; ISO 14126:1999; International Organization for Standardization: Geneva, Switzerland, 1999.
55. ASTM Standard. *Standard Test Method for Compressive Properties of Polymer Matrix Composite Materials*; ASTM D3410/D3410M; ASTM International: West Conshohocken, PA, USA, 2016.
56. ISO Standard. *Fibre-Reinforced Plastic Composites Determination of Apparent Interlaminar Shear Strength by Short-Beam Method*; ISO 14130:1997; International Organization for Standardization: Geneva, Switzerland, 1997.
57. ISO Standard. *Fibre-Reinforced Plastic Composites—Determination of the Stress/Shear Strain Response, Including the In-Plane Shear Modulus and Strength by the ±45° Tension Test Method*; ISO 14129:1997; International Organization for Standardization: Geneva, Switzerland, 1997.
58. ASTM Standard. *Standard Test Method for Open-Hole Tensile Strength of Polymer Matrix Composite Laminates*; ASTM D5766/D5766M-11; ASTM International: West Conshohocken, PA, USA, 2008.
59. ASTM Standard. *Standard Test Method for Open-Hole Compressive Strength of Polymer Matrix*; ASTM D6484/D6484M-20; ASTM International: West Conshohocken, PA, USA, 2009.
60. ASTM International. *Standard Practice for Filled-Hole Tension and Compression Testing of Polymer Matrix Composite Laminates*; ASTM D6742/D6742M-17; ASTM International: West Conshohocken, PA, USA, 2017.
61. UNE Standard. *Aerospace Series—Carbon Fibre Reinforced Plastics—Test Method—Determination of Interlaminar Fracture Toughness Energy—Mode I—GIC*; UNE-EN 6033:2015; Spanish Association for Standardization (UNE): Madrid, Spain, 2015.
62. UNE Standard. *Aerospace Series—Carbon Fibre Reinforced Plastics—Test Method—Determination of Interlaminar Fracture Toughness Energy—Mode II—GIIC (Endorsed by AENOR in January of 2016*; UNE-EN 6034:2015; Spanish Association for Standardization (UNE): Madrid, Spain, 2015.

63. ISO Standard. *Plastics—Differential Scanning Calorimetry (DSC)—Part 2: Determination of Glass Transition Temperature and Step Height*; ISO 11357-2:2020; International Organization for Standardization: Geneva, Switzerland, 2020.
64. Hexcel Corporation. HexFlow® RTM6. 2018. Available online: https://www.hexcel.com/user_area/content_media/raw/RTM6_DataSheetPDF.pdf (accessed on 3 August 2021).
65. Matsuhisa, Y.; Bunsell, A. Tensile failure of carbon fibers. In *Handbook of Tensile Properties of Textile and Technical Fibres*; Elsevier: Amsterdam, The Netherlands, 2009; pp. 574–602.
66. Jeon, Y.-P.; Alway-Cooper, R.; Morales, M.; Ogale, A.A. Carbon Fibers. In *Handbook of Advanced Ceramics*; Elsevier: Amsterdam, The Netherlands, 2013; pp. 143–154.
67. Composite Materials Database 900GPa.com. Product Datashhet: HEXCEL HexForce® G0926 D 1304 TCT. Available online: https://www.900gpa.com/es/product/fabric/WovenCombo_00A23AD07F?u=metric (accessed on 8 February 2022).
68. Teijin. Tenax Filament Yarn. Available online: https://www.teijincarbon.com/fileadmin/PDF/Datenblätter_en/Product_Data_Sheet_TSG01en__EU_Filament_.pdf (accessed on 8 February 2022).
69. Delasi, R.; Whiteside, J. Effect of Moisture on Epoxy Resins and Composites. In *Advanced Composite Materials—Environmental Effects*; ASTM International: West Conshohocken, PA, USA, 2009; p. 2.
70. Cauich-Cupul, J.I.; Pérez-Pacheco, E.; Valadez-Gonzalez, A.; Herrera-Franco, P.J. Effect of moisture absorption on the micromechanical behavior of carbon fiber/epoxy matrix composites. *J. Mater. Sci.* **2011**, *46*, 6664–6672, https://doi.org/10.1007/s10853-011-5619-0.
71. Liu, T.; Peng, J.; Liu, J.; Hao, X.; Guo, C.; Ou, R.; Liu, Z.; Wang, Q. Fully recyclable, flame-retardant and high-performance carbon fiber composites based on vanillin-terminated cyclophosphazene polyimine thermosets. *Compos. Part B Eng.* **2021**, *224*, 109188, https://doi.org/10.1016/j.compositesb.2021.109188.
72. Aranberri, I.; Landa, M.; Elorza, E.; Salaberria, A.M.; Rekondo, A. Thermoformable and recyclable CFRP pultruded profile manufactured from an epoxy vitrimer. *Polym. Test.* **2021**, *93*, 106931, https://doi.org/10.1016/j.polymertesting.2020.106931.
73. Hamada, H.; Oya, N.; Yamashita, K.; Maekawa, Z.-I. Tensile Strength and its Scatter of Unidirectional Carbon Fibre Reinforced Composites. *J. Reinf. Plast. Compos.* **1997**, *16*, 119–130, https://doi.org/10.1177/073168449701600202.
74. Maurin, R.; Davies, P.; Baral, N.; Baley, C. Transverse Properties of Carbon Fibres by Nano-Indentation and Micro-mechanics. *Appl. Compos. Mater.* **2008**, *15*, 61–73, https://doi.org/10.1007/s10443-008-9057-3.
75. Beylergil, B.; Tanoğlu, M.; Aktaş, E. Effect of polyamide-6,6 (PA 66) nonwoven veils on the mechanical performance of carbon fiber/epoxy composites. *Compos. Struct.* **2018**, *194*, 21–35, https://doi.org/10.1016/j.compstruct.2018.03.097.
76. Beylergil, B.; Tanoğlu, M.; Aktaş, E. Enhancement of interlaminar fracture toughness of carbon fiber-epoxy composites using polyamide-6,6 electrospun nanofibers. *J. Appl. Polym. Sci.* **2017**, *134*, 1–12, https://doi.org/10.1002/app.45244.
77. Quan, D.; Bologna, F.; Scarselli, G.; Ivankovic, A.; Murphy, N. Interlaminar fracture toughness of aerospace-grade carbon fibre reinforced plastics interleaved with thermoplastic veils. *Compos. Part A Appl. Sci. Manuf.* **2020**, *128*, 105642, https://doi.org/10.1016/j.compositesa.2019.105642.
78. García-Rodríguez, S.; Costa, J.; Rankin, K.; Boardman, R.; Singery, V.; Mayugo, J. Interleaving light veils to minimise the trade-off between mode-I interlaminar fracture toughness and in-plane properties. *Compos. Part A Appl. Sci. Manuf.* **2020**, *128*, 105659, https://doi.org/10.1016/j.compositesa.2019.105659.
79. Quan, D.; Bologna, F.; Scarselli, G.; Ivanković, A.; Murphy, N. Mode-II fracture behaviour of aerospace-grade carbon fibre/epoxy composites interleaved with thermoplastic veils. *Compos. Sci. Technol.* **2020**, *191*, 108065, https://doi.org/10.1016/j.compscitech.2020.108065.
80. Monteserín, C.; Blanco, M.; Murillo, N.; Pérez-Márquez, A.; Maudes, J.; Gayoso, J.; Laza, J.M.; Aranzabe, E.; Vilas, J.L. Effect of Different Types of Electrospun Polyamide 6 Nanofibres on the Mechanical Properties of Carbon Fibre/Epoxy Composites. *Polymers* **2018**, *10*, 1190, https://doi.org/10.3390/polym10111190.
81. Quan, D.; Alderliesten, R.; Dransfeld, C.; Murphy, N.; Ivanković, A.; Benedictus, R. Enhancing the fracture toughness of carbon fibre/epoxy composites by interleaving hybrid meltable/non-meltable thermoplastic veils. *Compos. Struct.* **2020**, *252*, 112699, https://doi.org/10.1016/j.compstruct.2020.112699.
82. Quan, D.; Deegan, B.; Alderliesten, R.; Dransfeld, C.; Murphy, N.; Ivanković, A.; Benedictus, R. The influence of interlayer/epoxy adhesion on the mode-I and mode-II fracture response of carbon fibre/epoxy composites interleaved with thermoplastic veils. *Mater. Des.* **2020**, *192*, 108781, https://doi.org/10.1016/j.matdes.2020.108781.
83. Cheng, C.; Chen, Z.; Huang, Z.; Zhang, C.; Tusiime, R.; Zhou, J.; Sun, Z.; Liu, Y.; Yu, M.; Zhang, H. Simultaneously improving mode I and mode II fracture toughness of the carbon fiber/epoxy composite laminates via interleaved with uniformly aligned PES fiber webs. *Compos. Part A Appl. Sci. Manuf.* **2020**, *129*, 105696, https://doi.org/10.1016/j.compositesa.2019.105696.
84. Daelemans, L.; van der Heijden, S.; De Baere, I.; Rahier, H.; Van Paepegem, W.; De Clerck, K. Nanofibre bridging as a toughening mechanism in carbon/epoxy composite laminates interleaved with electrospun polyamide nanofibrous veils. *Compos. Sci. Technol.* **2015**, *117*, 244–256, https://doi.org/10.1016/j.compscitech.2015.06.021.
85. Ramirez, V.A.; Hogg, P.J.; Sampson, W. The influence of the nonwoven veil architectures on interlaminar fracture toughness of interleaved composites. *Compos. Sci. Technol.* **2015**, *110*, 103–110, https://doi.org/10.1016/j.compscitech.2015.01.016.
86. Zhu, L. Investigations on damage resistance of carbon fiber composite panels toughened using veils. *Chin. J. Aeronaut.* **2013**, *26*, 807–813, https://doi.org/10.1016/j.cja.2013.05.006.

87. García-Rodríguez, S.; Costa, J.; Singery, V.; Boada, I.; Mayugo, J.A. The effect interleaving has on thin-ply non-crimp fabric laminate impact response: X-ray tomography investigation. *Compos. Part A Appl. Sci. Manuf.* **2018**, *107*, 409–420, https://doi.org/10.1016/j.compositesa.2018.01.023.
88. Wu, Z.; Yi, X.-S.; Wilkinson, A. Interlaminar fracture toughness of carbon fibre/RTM6-2 composites toughened with thermoplastic-coated fabric reinforcement. *Compos. Part B Eng.* **2017**, *130*, 192–199, https://doi.org/10.1016/j.compositesb.2017.08.003.
89. Beckermann, G.W.; Pickering, K. Mode I and Mode II interlaminar fracture toughness of composite laminates interleaved with electrospun nanofibre veils. *Compos. Part A Appl. Sci. Manuf.* **2015**, *72*, 11–21, https://doi.org/10.1016/j.compositesa.2015.01.028.
90. Kuwata, M.; Hogg, P. Interlaminar toughness of interleaved CFRP using non-woven veils: Part Mode-II testing. *Compos. Part A Appl. Sci. Manuf.* **2011**, *42*, 1560–1570, https://doi.org/10.1016/j.compositesa.2011.07.017.